archives
of thermodynamics
Vol. 39(2018), No. 2, 97–122
DOI: 10.1515/aoter-2018-0014

Thermal analysis of generalized Burgers nanofluid over a stretching sheet with nonlinear radiation and non uniform heat source/sink

K. GANESH KUMAR[1]
G.K. RAMESH[2*]
B.J. GIREESHA[1]

[1] Department of Studies and Research in Mathematics, Kuvempu University, Shankaraghatta-577 451, Shimoga, Karnataka, India

[2] Department of Mathematics, K.L.E Society's J.T. College, Gadag 582102, Karnataka, India

Abstract The work deals with the heat analysis of generalized Burgers nanofluid over a stretching sheet. The Rosseland approximation is used to model the non-linear thermal radiation and incorporated non-uniform heat source/sink effect. The governing equations reduced to a set of nonlinear ordinary differential equations under considering the suitable similarity transformations. The obtained ordinary differential equations equations are solved numerically by Runge-Kutta-Fehlberg order method. The effect of important parameters on velocity, temperature and concentration distributions are analyzed and discussed through the graphs. It reveals that temperature increases with the increase of radiation and heat source/sink parameter.

Keywords: Burgers nanofluid; Non-uniform heat source/sink; Non-linear radiation; Magnetic field; Stretching surface

Nomenclature

A_1	–	rate of strain tensor
A, B	–	heat generation or absorption

*Corresponding Author. Email: gkrmaths@gmail.com

b	–	constants
B_0	–	magnetic field
C	–	nanoparticle volume fraction, kg/m^3
C_w	–	concentration at the wall
C_∞	–	ambient nanofluid volume fraction, kg/m^3
c_p	–	specific heat coefficient, J/kg K
D_B	–	Brownian diffusion coefficient
D_T	–	thermophoretic diffusion coefficient
k	–	thermal conductivity, W/m K
k^*	–	mean absorption coefficient, m^{-1}
L	–	velocity gradient
Le	–	Lewis number
M	–	magnetic parameter
Nb	–	Brownian motion parameter
Nt	–	thermophoresis parameter
Nu_x	–	local Nusselt number
q'''	–	non-uniform heat source/sink
q_w	–	surface shear stress
q_m	–	surface heat flux
Pr	–	Prandtl number
q_r	–	radiation heat flux, Wm^{-2}
R	–	radiation parameter
Re_x	–	local Reynolds number
S	–	extra stress tensor
Sh_x	–	local Sherwood number q'''
T	–	fluid temperature, K
T_w	–	surface temperature, K
T_∞	–	ambient surface temperature, K
t	–	time
u, v	–	velocity components, m/s^{-1}
U_w	–	stretching sheet
x, y	–	coordinates, m

Greek symbols

α	–	thermal diffusivity
β_1, β_2	–	Deborah numbers in terms of relaxation time
β_3	–	Deborah number in terms of retardation time
η	–	similarity independent variable
θ	–	dimensionless temperature
θ_w	–	temperature ratio parameter
λ_1, λ_2	–	relaxation time
λ_3	–	retardation time
μ_1	–	dynamic viscosity, Ns/m^2
ν	–	kinematic viscosity of the fluid, m^2 s^{-1} K
ρ	–	density of fluid
σ	–	electrical conductivity

τ	–	ratio of the effective heat capacity of the nanoparticle to that of an ordinary fluid
ϕ	–	dimensionless nanoparticle volume fraction
ψ	–	stream function

1 Introduction

In recent years the study of heat and mass transfer on magnetohydrodynamics (MHD) flows has a variety of applications in engineering and industry especially in meteorology, solar physics, cosmic fluid dynamics, astrophysics, geophysics and in the motion of earth's core, nuclear reactors, polymer production and food processing, liquid metal heat exchangers, geophysics and astrophysics. In view of these applications, Gupta and Gupta [1] discussed the heat and mass transfer on a stretching sheet with suction and blowing. Chan and Char [2] analyzed the heat and mass transfer on a continuous stretching sheet with suction and blowing. Makinde *et al.* [3] studied the buoyancy effect on a stagnation point MHD flow of nanofluid with convective condition. Rashidi *et al.* [4] examined the radiation and buoyancy effects on a Newtonian fluid past a vertical surface. Das *et al.* [5] presents the heat and mass effects on a second order fluid with convective boundary condition. Ramesh *et al.* [6–8] reported the two-phase dusty liquid flow over a permeably moving sheet under various aspects and conditions.

The study of nanofluids is gaining a lot of attention due to its vast applications in nuclear energy, medicine, space exploration, ethylene glycol, engine oil in high technological areas and heat transfer in high technological industries etc. Accordingly, Choi [9] was the first who introduced the term nanofluid indicating engineered colloids composed of nanoparticles dispersed in a base fluid. Comprehensive survey of convective transport in nanofluid has been investigated by Buongiorno [10]. Flow of nanofluid past a stretching sheet was first analyzed by Khan and Pop [11]. Alsaedi *et al.* [12] discussed the effect of heat generation/absorption on the stagnation point flow of nanofluid towards an impermeable stretching surface. Using high-level language and interactive environment Rahman *et al.* [13] elaborate convection flow of water based nanofluid past a wedge and studied the effects of magnetic field and heat source/sink. Nandy and Mahapatra [14] obtained the solutions of stagnation point flow over a stretching/shrinking sheet via shooting technique. Some recent investigations on nanofluid with different geometries are consulted in [15–19].

Presently, non-Newtonian fluids have a numerous applications in industry and technology, e.g., food, chemical, biological and pharmaceutical industries, drilling muds, apple sauce, paper pulp, paints, polymer solutions, certain oils, and clay coating, etc. The behavior of non-Newtonian liquids the foremost equations become more complex to handle as extra nonlinear terms appear in the equation of motion. Predominantly, reaction of numerous viscoelastic fluids can be caught sensibly well by the rate type fluid models. The fluid model under thought is a subclass of the rate-type fluid that is known as the generalized Burgers fluid. Consequently, a thermodynamic framework has been put into place to develop a one-dimensional model due to Burgers [20] to the frame indifferent of three dimensional forms by Rajagopal and Srinivasa [21]. The Burgers model has been successfully used to describe the response of asphalt and asphalt concrete [22] as well as used to model the geological structures like Olivine rocks [23]. In spite of diverse applications, the Burgers model has not been given due attention. Khan and Khan applied the homotopy analysis method (HAM) to obtain the generalized Burgers fluid in the presence of nanoparticles [24]. Hayat *et al.* studied the heat and mass transfer effect on inclined surface of Burgers fluid [25]. This model has been inspected by a few researchers [26–31]. Another important aspect of heat transport phenomenon which attained the special focus is called thermal radiation. The suitable knowledge of heat transfer via radiation is essential for the achievement of best quality products in industry. Several engineering processes include space vehicles, hypersonic fights, gas turbines, nuclear power plants, etc. involve the phenomenon of radiation. Nowadays, radiative heat transport has also role in the techniques of renewable energy. Various researches have been done to describe the mechanism of radiation [32–37].

Based on the above studies, here our plan is to elaborate the features of radiation and non-uniform heat source/sink in Burgers nanoliquid flow generated by stretched surface. We also utilized the concept of non-linear radiation phenomenon. Numerical computation is made to find the solution of non-linear governed expressions. The results of dimensionless quantities have been visualized for various values of emerging physical constraints.

2 Mathematical formulation

The fundamental equations of mass, momentum, energy and nanoparticles of the flow yield, Khan and Khan [24]

$$\nabla \cdot V = 0\,, \tag{1}$$

$$\rho(V \cdot \nabla) = -\nabla p + \nabla \cdot S \,, \tag{2}$$

$$(V \cdot \nabla)T = \alpha \nabla^2 T + \tau \left(D_B \nabla C \cdot \nabla T + \frac{D_T}{T_\infty} \nabla T \cdot \nabla T \right) \,, \tag{3}$$

$$(V \cdot \nabla)C = D_B \nabla^2 C + \frac{D_T}{T_\infty} \nabla^2 T \,, \tag{4}$$

where V is the velocity vector, p is the pressure, T is the temperature, S is the stress field, ρ is the density, D_T, D_B denote thermophoresis diffusion coefficient, Brownian diffusion coefficient, respectively. The extra stress tensor for incompressible generalized Burgers fluid is related to the motion of fluid satisfies the constitutive equation as (see Hayt *et al.* [25])

$$S + \lambda_1 \frac{DS}{Dt} + \lambda_2 \frac{D^2 S}{Dt^2} = \mu_1 \left[A_1 + \lambda_3 \frac{DA_1}{Dt} \right] \,, \tag{5}$$

where μ_1 is the dynamic viscosity, A_1 is the rate of strain tensor, λ_1 and λ_2 are the relaxation time, and λ_3 is the retardation time, $\frac{D}{Dt}$ denotes the upper convected derivative defined as (see Khan and Khan [24])

$$\frac{Da_i}{Dt} = \frac{\partial a_i}{\partial t} + u_r a_{i,r} - u_{i,r} a_r \,, \tag{6}$$

in which $\frac{d}{dt}$ is the material time derivative, t is the time, $a_{i,r}$, a_r, $u_{i,r}$, u_r denote tensor property of a small parcel of fluid.

Stress fields are of the form

$$V = \Big[u(x,y), v(x,y), 0 \Big], \quad T = T(x,y), \quad C = C(x,y), \quad S = S(x,y) \,. \tag{7}$$

Noted that Burgers' fluid model reduces to the special cases of the Oldroyd-B model, Maxwell model and the Newtonian fluid model when $\lambda_2 = 0$, $\lambda_2 = \lambda_3 = 0$ and $\lambda_1 = \lambda_2 = \lambda_3 = 0$, respectively.

In the present work, following assumptions have been made:

1. The two-dimensional steady, incompressible flow of generalized Burgers nanofluid over a stretching sheet is considered.
2. The x-axis is assumed to be along the stretching sheet and y-axis is assumed to be normal to it (see Fig. 1).

3. The flow is induced due to the linear stretching of sheet varying with distance x, i.e., $U_w = bx$ here b is a real positive number and x is the coordinate measured from the location where the sheet velocity is zero.

4. Thermophoresis and Brownian motion effects are also taken into account.

5. Magnetic field of strength B_0 is applied in transverse direction to the flow.

6. T_w is the surface temperature at the wall, C_w is the solutal concentration. At large distance from the sheet, temperature, nanoparticle concentrations are represented by T_∞ and C_∞, respectively.

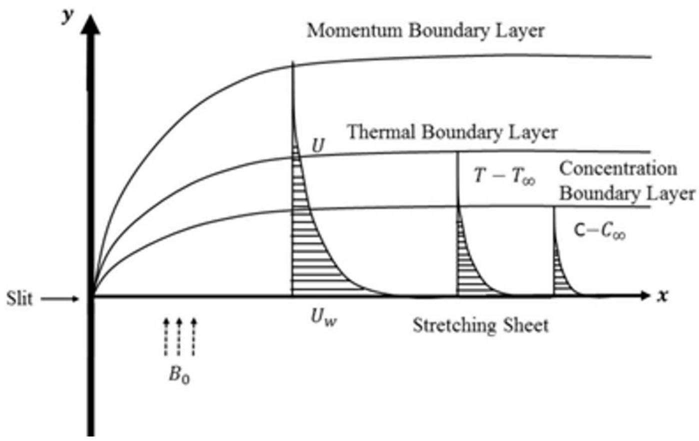

Figure 1: Physical model of the problem.

Making use of (7) into (1) to (4), Under the boundary layer approximation, the velocity, temperature and concentration fields are governed by the following equations, Hayat *et al.* [25]:

$$\frac{\partial u}{\partial x} + \frac{\partial v}{\partial y} = 0 \,, \tag{8}$$

$$
\begin{aligned}
&u\frac{\partial u}{\partial x}+v\frac{\partial u}{\partial y}+\lambda_1\left(u^2\frac{\partial^2 u}{\partial x^2}+v^2\frac{\partial^2 v}{\partial y^2}+2uv\frac{\partial^2 u}{\partial x\partial y}\right)\\
&+\lambda_2\left[\begin{array}{c}
u^3\frac{\partial^3 u}{\partial x^3}+v^3\frac{\partial^3 u}{\partial y^3}+u^2\left(\frac{\partial u}{\partial x}\frac{\partial^2 u}{\partial x^2}-\frac{\partial u}{\partial y}\frac{\partial^2 v}{\partial y^2}+2\frac{\partial v}{\partial x}\frac{\partial^2 u}{\partial x\partial y}\right)\\
+3v^2\left(\frac{\partial v}{\partial y}\frac{\partial^2 u}{\partial y^2}+\frac{\partial u}{\partial y}\frac{\partial^2 u}{\partial x\partial y}\right)+3uv\left(u\frac{\partial^2 u}{\partial x^2\partial y}+v\frac{\partial^2 u}{\partial x\partial y^2}\right)\\
+2uv\left(2\frac{\partial u}{\partial y}\frac{\partial^2 u}{\partial x^2}+\frac{\partial v}{\partial x}\frac{\partial^2 u}{\partial y^2}+\frac{\partial v}{\partial y}\frac{\partial^2 u}{\partial x\partial y}\right)
\end{array}\right] \qquad (9)\\
&=\upsilon\frac{\partial^2 u}{\partial y^2}+\upsilon\lambda_3\left(u\frac{\partial^2 u}{\partial y^2\partial x}+v\frac{\partial^3 u}{\partial y^3}-\frac{\partial u}{\partial x}\frac{\partial^2 u}{\partial y^2}-\frac{\partial u}{\partial y}\frac{\partial^2 v}{\partial y^2}\right)-\frac{\sigma B_0}{\rho}u\,,
\end{aligned}
$$

$$
u\frac{\partial T}{\partial x}+\frac{\partial T}{\partial y}=\alpha\frac{\partial^2 T}{\partial y^2}+\tau\left(D_B\frac{\partial C}{\partial y}\frac{\partial T}{\partial y}+\frac{D_T}{T_\infty}\left(\frac{\partial T}{\partial y}\right)^2\right)-\frac{\partial q_r}{\partial y}+q''' \,, \qquad (10)
$$

$$
u\frac{\partial C}{\partial x}+\frac{\partial C}{\partial y}=D_B\frac{\partial^2 C}{\partial y^2}+\frac{D_T}{T_\infty}\frac{\partial^2 T}{\partial y^2}, \qquad (11)
$$

with the relevant boundary conditions

$$
\begin{aligned}
&u=U_w(x),\quad v=0,\quad T=T_w,\quad C=C_w \text{ at } y=0\,,\\
&u\to 0,\ T\to T_\infty,\ C\to C_\infty \quad \text{at}\ \ y\to\infty \qquad (12)
\end{aligned}
$$

where u and v represent the velocity components in the x and y directions, respectively, α – the thermal diffusivity, $\upsilon=\frac{\mu}{\rho}$ is kinematic viscosity, ρ is density of fluid, σ is the electrical conductivity, whereas τ denotes the ratio of effective heat capacity of the nanoparticle material to the heat capacity of the fluid, D_B the Brownian diffusion coefficient and D_T the thermophoresis diffusion coefficient, q_r is the radiative heat flux, q''' is the non-uniform heat source/sink, where q''' is the space and temperature dependent heat generation/absorption which can be expressed as

$$
q'''=\frac{kU_w}{x\upsilon}\Big[A(T_w-T_\infty)+B(T-T_\infty)\Big]\,, \qquad (13)
$$

where A and B are parameters of space and temperature dependent heat generation or absorption. Here, if $A>0$ and $B>0$ corresponds to internal heat generation, whereas $A<0$ and $B<0$ corresponds to internal heat absorption.

Using the Rosseland approximation for radiation, radiation heat flux is simplified as

$$
q_r=-\frac{4\sigma^*}{3k^*}\frac{\partial T^4}{\partial y}=-\frac{16\sigma^*}{3k^*}T^3\frac{\partial T}{\partial y}\,, \qquad (14)
$$

where σ^* is the Stefan–Boltzmann constant and k^* is the mean absorption coefficient.

Now after simplification Eq. (10) takes the form

$$u\frac{\partial T}{\partial x}+\frac{\partial T}{\partial y}=\frac{\partial}{\partial y}\left[\alpha+\frac{16\sigma^* T_\infty^3}{3k^*}\right]\frac{\partial T}{\partial y}+\tau\left[D_B\frac{\partial C}{\partial y}\frac{\partial T}{\partial y}+\frac{D_T}{T_\infty}\left(\frac{\partial T}{\partial y}\right)^2\right]+q''' . \tag{15}$$

We introduce the change of variables as follows:

$$\varphi=\Big(\upsilon x u_w(x)\Big)^{\frac{1}{2}}f(\eta),\qquad T=T_\infty(1+(\theta_w-1)\theta),$$

$$\phi(\eta)=\frac{C-C_\infty}{C_w-C_\infty},\qquad \eta=\left(\frac{u_w(x)}{\upsilon x}\right), \tag{16}$$

where $\theta_w=\frac{T_w}{T_\infty},\theta_w>1$ being the temperature ratio parameter. Where φ the stream function is defined as

$$u=\frac{\partial\varphi}{\partial y}\ \text{ and }\ v=-\frac{\partial\varphi}{\partial x} \tag{17}$$

Now using Eqs. (16) and (17), Eq. (8) is identically satisfied and Eqs. (9), (11) and (15) yield

$$f'''+ff''-f'^2+\beta_1\Big(2ff'f''-f^2f''')+\Big)\beta_2(f^3f'''-2ff'^2f''-3f^2f''^2)$$

$$+\beta_3(f''^2-ff''')-Mf'=0\,, \tag{18}$$

$$\Big[1+\frac{4}{3}R\frac{d}{d\eta}(1+(\theta_w-1)\theta)^3\Big]\theta''+\Pr f\theta'+Nb\theta'\phi'+Nt\theta'^2+Af'+B\theta=0\,, \tag{19}$$

$$\phi''+\mathrm{Le}\,f\phi'+\frac{Nt}{Nb}\theta''=0\,, \tag{20}$$

with the boundary condition:

$$f=0,\ f'=1,\ \theta=1,\ \phi=1\ \text{ as }\ \eta=0\,,$$

$$f'=0,\ \theta\to0,\ \phi\to0\ \text{ as }\ \eta\to\infty\,, \tag{21}$$

where $\beta_1=\lambda_1 b$ and $\beta_2=\lambda_2 b^2$ are the Deborah numbers in terms of relaxation time respectively, $\beta_3=\lambda_3 b$ is the Deborah number in terms of retardation time, $R=\frac{4\sigma^* T_\infty^3}{kk^*}$ is the radiation parameter. $\Pr=\frac{\upsilon}{\alpha}$ is the Prandtl number, $\mathrm{Le}=\frac{\alpha}{D_B}$is the Lewis number, $Nb=\frac{\tau D_B(C_w-C_\infty)}{\upsilon}$ is the Brownian motion parameter, $Nt = \frac{\tau D_T(T_w - T_\infty)}{T_\infty v}$ is the thermophoresis parameter. The symbols: prime, double prime, etc. denote first order derivative, second order derivative, respectively.

The local Nusselt number (Nu_x) and local Sherwood number (Sh_x) are

$$\mathrm{Nu}_x = \frac{U_w q_w}{kb(T_w - T_\infty)} \quad \text{and} \quad \mathrm{Sh}_x = \frac{U_w q_m}{D_m b(C_w - C_\infty)}$$

where the surface shear stress q_w and the surface heat flux q_m are given by

$$q_w = -k\left(\frac{\partial T}{\partial y} + q_r\right)_{y=0} \quad \text{and} \quad j_w = -D_m\left(\frac{\partial C}{\partial y}\right)_{y=0} .$$

Using similarity transformations we get

$$\mathrm{Nu}_x(\mathrm{Re}_x)^{-\frac{1}{2}} = \left[1 + \frac{4}{3}R\theta_w^3\right]\theta'(0) \ \text{ and } \ \mathrm{Sh}_x(\mathrm{Re}_x)^{\frac{1}{2}} = -\phi'(0) ,$$

where the local Reynolds number has been defined as $\mathrm{Re}_x = \frac{x\,U_w(x)}{v}$ (see Khan and Khan [24]).

3 Numerical method

Equations (18)–(20) are highly non-linear in nature, hence the exact solution does not seem to be feasible. Therefore, these equations with subject to boundary conditions (21) are solved numerically by Runge-Kutta-Fehlberg fourth-fifth order method (denoted RKF45) using a high-level language and interactive environment. In this package, two submethods are available, namely trapezoidal and midpoint method. To solve this kind of two point boundary value problem the trapezoidal method is generally efficient, but it is incapable to handle harmless end point singularities, but this can able in midpoint method. Thus, the midpoint method with the Richardson extrapolation enhancement scheme is chosen as a sub-method. Here first we reduced the given equations into system of seven first order simultaneous equations having seven unknowns as:

$$f' = y, \ \ f'' = y_1, \ \ f''' = y_2, \ \ f'''' = y_3 ,$$

$$y_3 = -(fy_1 + y^2 + \beta_1(2fyy_1 - f^2y_2) + \beta_2(f^3y_2 - 2fy^2y_2 - 3f^2y_1^2) \\ +\beta_3(y_1^2 - fy_2) - My) ,$$

$$\theta' = z, \quad \theta'' = z_1 \,,$$

$$z_1 = -\left(\frac{1}{1+\frac{4}{3}R\frac{d}{d\eta}(1+(\theta_w-1)\theta}\right)(\Pr fz + Nb\,zq + Nt\,z^2 + Ay + B\theta)\,,$$

$$\phi' = q, \quad \phi'' = q_1 \,,$$

$$q = -\left(\mathrm{Le}\,fq + \frac{Nt}{Nb}q_1\right)\,,$$

with the corresponding conditions as

$$f = 0\,,\ y_1 = 1\,,\ \theta = 1\,,\ \phi = 1,\ \text{as}\ \ \eta = 0\,,$$
$$y_1 \to 0\,,\ \theta \to 0\,,\ \phi \to 0 \quad \text{at}\ \ \eta \to \infty\,.$$

The asymptotic boundary conditions at η_∞, were replaced by those at $\eta_\infty = 6$ in accordance with standard practice in the boundary layer analysis. Additionally, the relative error tolerance for convergence is considered to be 10^{-6} throughout our numerical computation. Further it is important to mention that as finding the solutions of velocity, temperature and concentration, the CPU time to estimate the values of velocity (1.58 s) is much less than the CPU time to evaluate the values of temperature (2.65 s) and the CPU (central processing unit) time (or processing time) for concentration is 2.90 s. To assess the accuracy of the aforementioned numerical method, comparison of skin friction coefficient and local Nusselt number values between the present results and existing results for various values presented in Tab. 1.

4 Results and discussion

To get a clear insight into the physical situation of the present problem, numerical values for velocity, temperature and concentration profile are computed for different values of dimensionless parameters using the method described in the previous section. The numerical results are tabulated and displayed with the graphical illustrations. Figures 2a and 2b demonstrate the effects of Deborah number, β_1, on the velocity profile. It is observed from this plot that the thickness of the momentum boundary layer is found

Table 1: Comparison results for the function $-f''(0)$ for several values of M in the case $\beta_1 = \beta_2 = \beta_3 = 0$, where M is the magnetic parameter.

M	$-f''(0)$		
	Cortell [38]	Ramesh *et al* [8]	Present result
0	1.000	1.000	1.00006
0.2	1.095	1.095	1.09546
0.5	1.224	1.224	1.22475
1	1.414	1.414	1.41421
1.2	1.483	1.483	1.48324
1.5	1.581	1.581	1.58114
2	1.732	1.732	1.73205

to decrease as Deborah number increases, which results in thicker boundary layer thickness. Physically, Deborah number is the ratio of relaxation to observation time. So with the enhancement in Deborah number the relaxation time also increases which provides more resistance to the fluid motion. Therefore, velocity profile diminishes. Figure 2b is the representation of velocity profile for various values of the Deborah number, β_2. It is evident that the large values of Deborah number results in thickening of thermal boundary layer. Figure 2c explores the effect of the Deborah number, β_3, on velocity profile. This figure reveals an increasing behavior of the velocity profile for larger values of the Deborah number. Physically, it is due to fact that Deborah number is dependent on the retardation time. Therefore the larger value of Deborah number increases the retardation time. Consequently, the fluid flow is accelerated.

Figures 3a and 3b are depicted for the variation of the non-uniform heat source/sink parameters, A, and, B, on temperature profiles. Apparently, these figures show increasing behavior of temperature profile with the larger values of the non-uniform heat source/sink parameters. It is also observed that the heat is generated for increasing values of $A > 0$ and $B > 0$ and this causes an increase in the heat transfer rate in both cases. The behaviors of magnetic parameter, M, on velocity, temperature and concentration distribution are sketched in Figs. 4a, 4b and 4c. From Fig. 4a it is found that

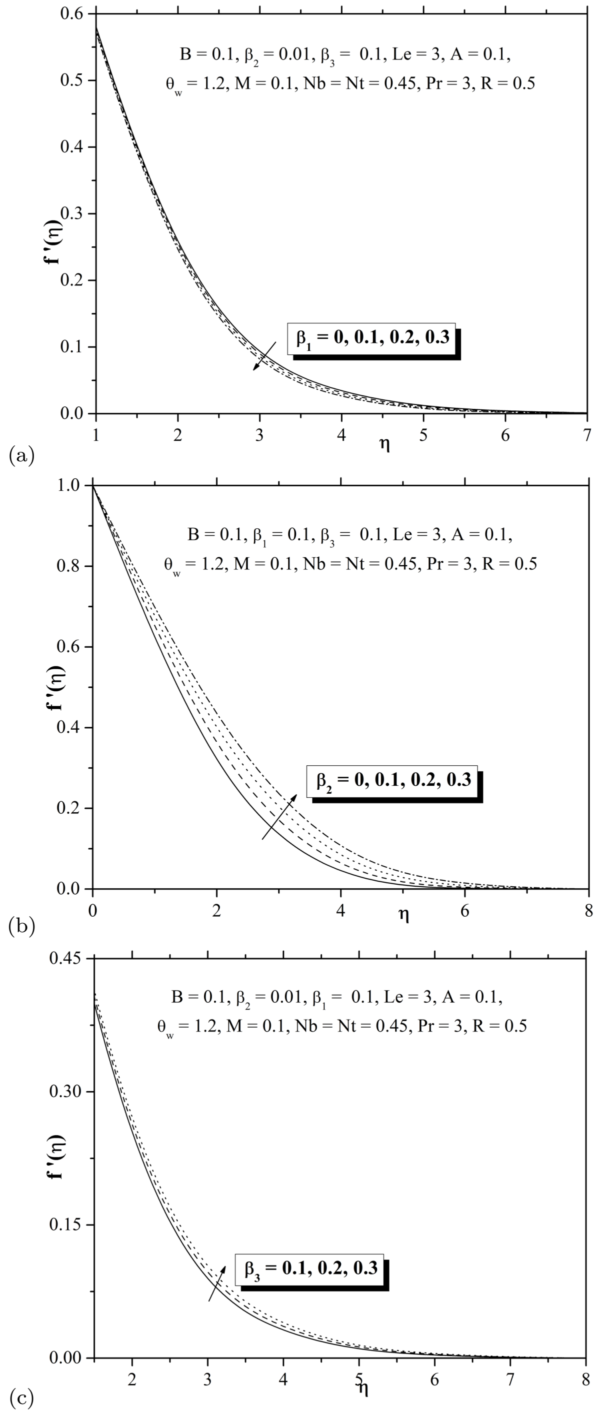

Figure 2: Influence of β_1 – (a) , β_2 – (b), β_3 – (c) on velocity profile.

Table 2: Variation of skin friction coefficient, Nusselt number , Nu_x, and Sherwood number, Sh_x, for different physical parameters.

A	B	θ_w	Le	M	Nb	Nt	Pr	R	β_1	β_2	β_3	$-\mathrm{Nu}_x\,\mathrm{Re}^{-1/2}$	$-\mathrm{Sh}_x\,\mathrm{Re}^{-1/2}$
0.1												0.55804	1.11075
0.2												0.51664	1.12339
0.3												0.47499	1.13612
	0											0.61274	1.09506
	0.1											0.55804	1.11075
	0.2											0.49993	1.12718
		1										0.48174	1.11477
		1.1										0.52193	1.11051
		1.2										0.55804	1.11075
			2									0.58802	0.82041
			3									0.55804	1.11075
			4									0.54213	1.34748
				0								0.56778	1.12409
				0.1								0.55804	1.11075
				0.2								0.54866	1.09808
					0.2							0.72721	0.89262
					0.4							0.61020	1.07640
					0.6							0.50978	1.13244
						0						0.72270	1.16499
						0.1						0.68551	1.14826
						0.2						0.65061	1.13488
							2					0.46902	1.11428
							3					0.55804	1.11075
							4					0.58908	1.11855
								0.5				0.55804	1.11075
								1				0.85678	1.11075
								1.5				0.99486	1.10318
									0			0.55869	1.11209
									0.1			0.55804	1.11075
									0.2			0.55722	1.10919
										0		0.57558	1.13516
										0.01		0.57516	1.13455
										0.02		0.57475	1.13394
											0.1	0.55804	1.11075
											0.2	0.56716	1.12334
											0.3	0.57516	1.13455

velocity and momentum boundary layer thickness increase with increase in magnetic parameter. This is due to the fact that the applied transverse magnetic field produces a force called the Lorentz force, which opposes the flow. This resistive force tends to slow down the flow, so the effect of M decreases the velocity and also causes increase in its temperature and con-

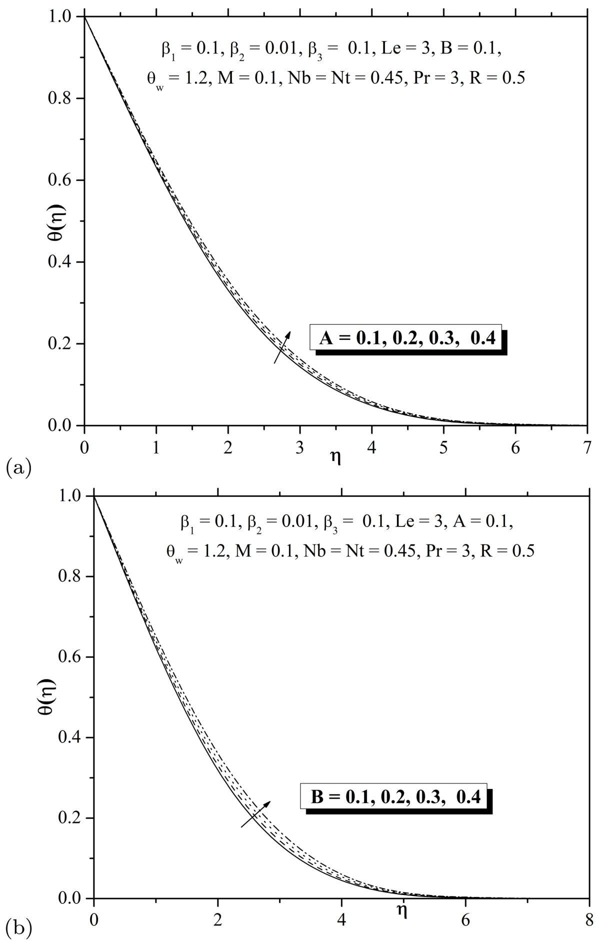

Figure 3: Influence of A – (a), B – (b) on temperature profile.

centration profile as shown in Figs. 4b and 4c. Furthermore, these figures lead to the conclusion that the thermal and solutal boundary layer thicknesses are increasing functions of the magnetic parameter.

The impact of Brownian motion parameter, Nb, on the temperature and concentration distributions is depicted through Figs. 5a and 5b. It is anticipated by the Fig. 5a that the temperature distribution increases as the Brownian motion parameter increases. As Brownian motion parameter increases, random motion of fluid particles increase which results in more heat production. Thus temperature profiles show increasing behavior

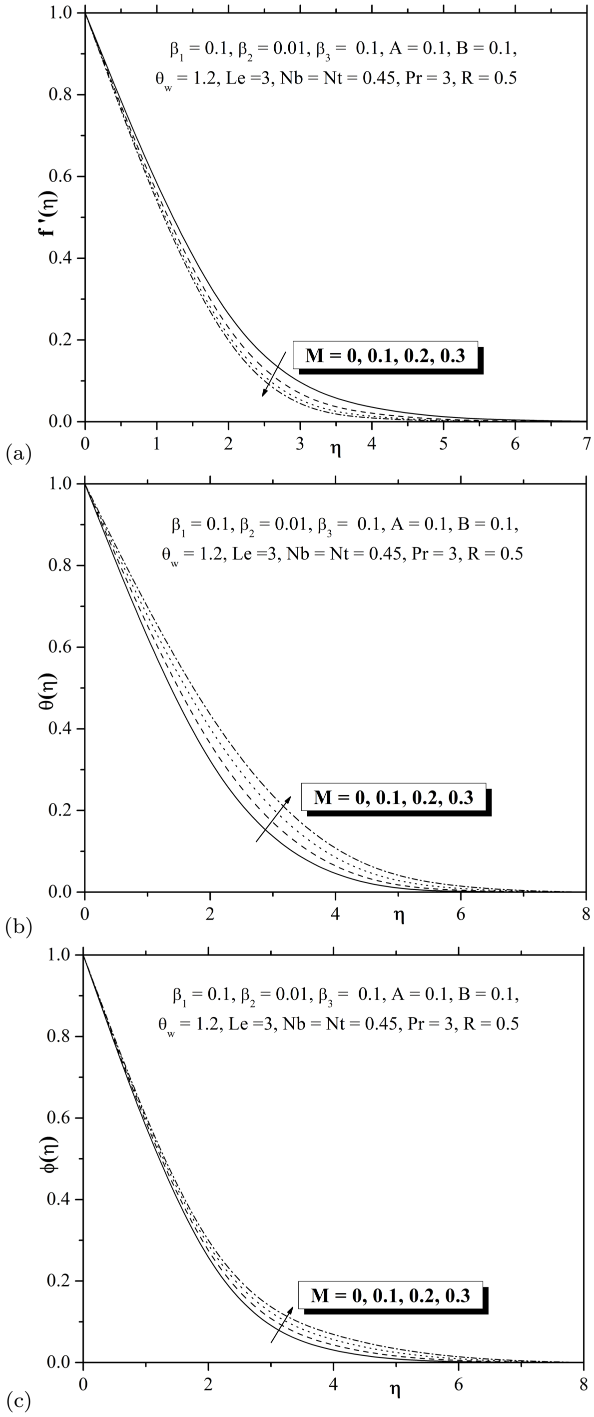

Figure 4: Influence of M on: a – velocity profile, b – temperature profile, c – concentration c.

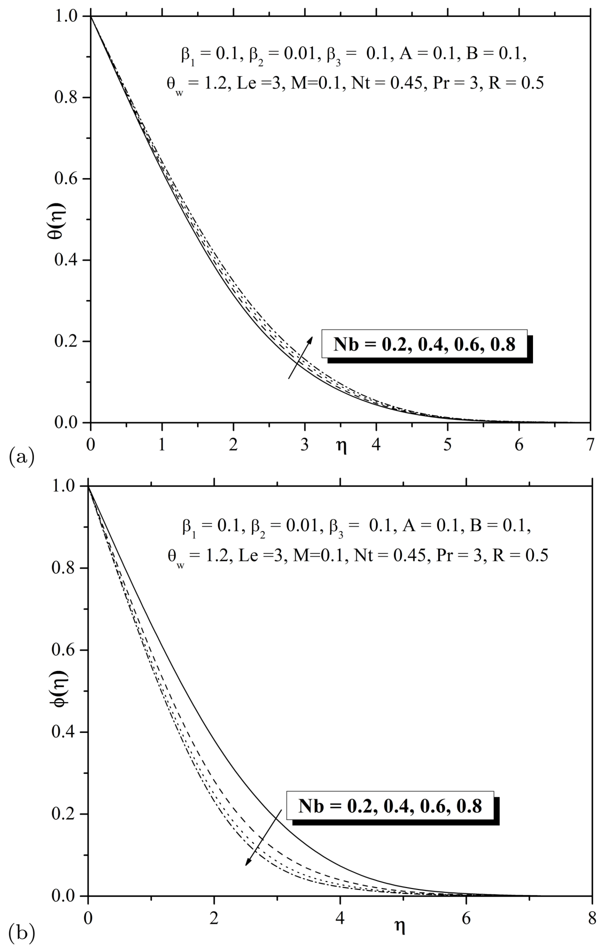

Figure 5: Influence of Nb on: a – temperature profile, b – concentration profile.

whereas the concentration profiles show opposite behavior. Figures 6a and 6b are plotted to see the effects of thermophoresis parameter, Nt, on the temperature and nanoparticle concentration profiles. It is clear that the larger value of thermophoresis parameter is to increase the temperature and nanoparticle concentration profiles. It is also found that the effect of thermophoresis parameter is also to intensify the heat transfer. Impact of temperature ratio parameter, θ_w, on the temperature profile is given in Fig. 7a, and it indicates that increase in temperature ratio parameter increases the temperature profile and corresponding boundary layer thick-

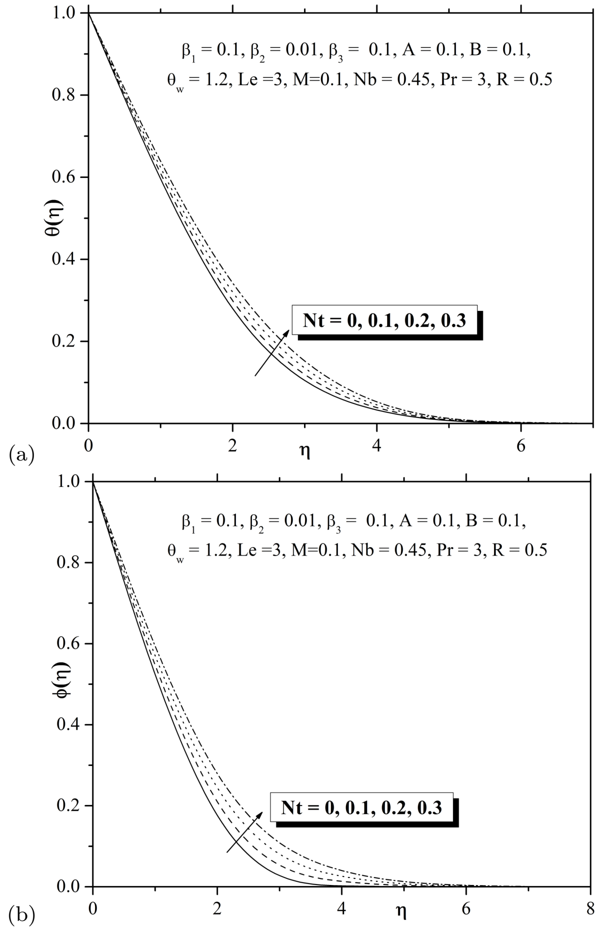

Figure 6: Influence of Nt on: a – temperature profile, b – concentration profile.

ness. Figure 7b describes the influences of radiation parameter, R, on the dimensionless temperature profile. The results are presented for four different values of radiation parameter. It is clear that the thermal boundary layer thickness increases for increasing values of radiation parameter. This is due to the fact that the increase in radiation parameter provides more heat to fluid that causes an enhancement in the temperature and thermal boundary layer thickness.

Figure 7c demonstrates the effect of Prandtl number, Pr, on temperature profile. It is noticed that, the temperature profile and corresponding thermal boundary layer depresses rapidly with increasing values of Pr.

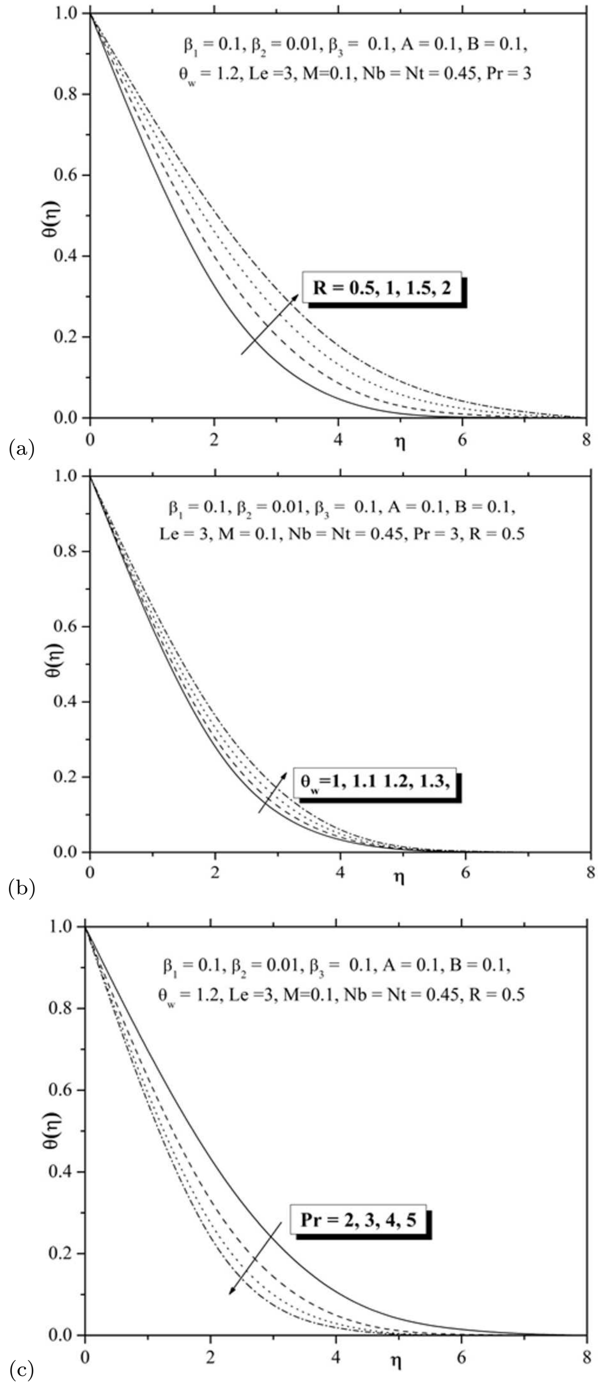

Figure 7: Influence of R on temperature profile – a, influence of θ on temperature profile – b, influence of Pr on temperature profile – c.

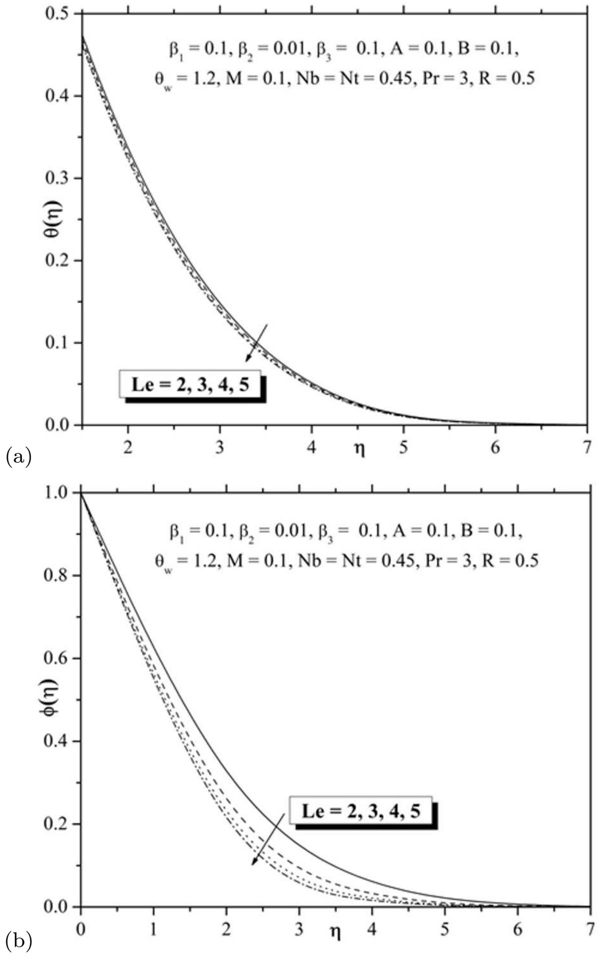

Figure 8: Influence of Le on temperature profile – a, concentration profile – b.

Physically, the Prandtl number is the ratio of momentum diffusivity to thermal diffusivity. In fact, the larger the value pf Prandtl number renders lower thermal diffusivity. A reduction in the thermal diffusivity leads to the decrease in temperature and its associated boundary layer thickness, which as can be shown in Fig. 7c. Figures 8a and 8b depicts the effect the Lewis number, Le, on temperature and concentration profiles, respectively. It is evidently observed that, the thermal and solutal boundary layer thickness decrease as Lewis number increases. The physical reason behind this is the increase in Lewis number implies decrease in solute diffusivity or

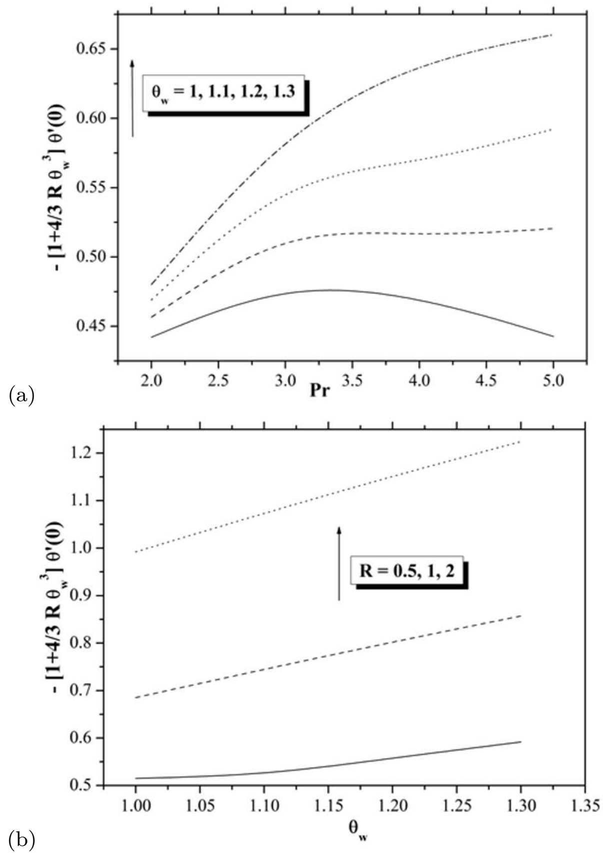

Figure 9: Influence of Pr and θ_w on Nusselt number – a, influence of θ_w and R on Nusselt number – b.

less Brownian diffusion and eventually less penetration depth for both rate of heat transfer and mass transfer rate. Figure 9a and 9b shows that the influence of θ_w and R versus Pr and θ_w parameters respectively on Nusselt number. It is noticed that the Nusselt number increases rapidly with increasing values of θ_w and R versus Pr and θ_w, respectively. Figure 10a and 10b are plotted to illustrate the effects of A and Nb versus B and Nt parameters respectively on local Nusselt number. The local Nusselt number decreases by increasing of A and Nb verses B and Nt parameters respectively. Figure 11a shows that the influence of R and Le parameter on the local Sherwood number. It is clear that the Sherwood number increases for increasing values of R and Le. Figure 11b and 11c depicts the variation of

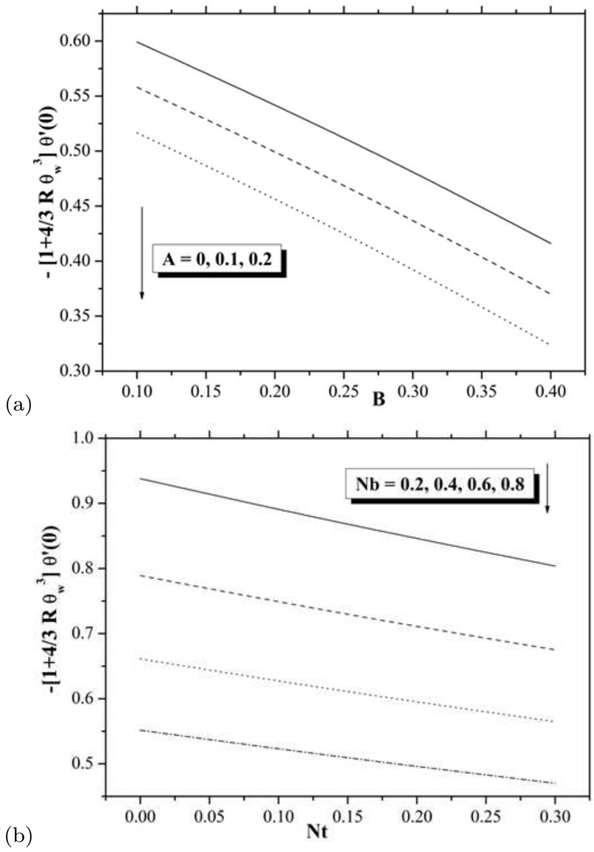

Figure 10: Influence of B and A on Nusselt number – a, influence of Nt and Nb on Nusselt number –b.

local Sherwood number in response to a change in Nb and Le versus Nt respectively. The graph shows that the local Sherwood number decreases as Nb and Le versus Nt respectively increase.

5 Conclusion

An analysis has been developed to investigate the boundary layer flow and heat transfer of generalized Burgers' nanofluid over the stretching sheet in the presence of non-linear radiation and non-uniform heat source sink. A comparison between the present numerical solutions with previously published results has been included, and the results are found to be in excellent

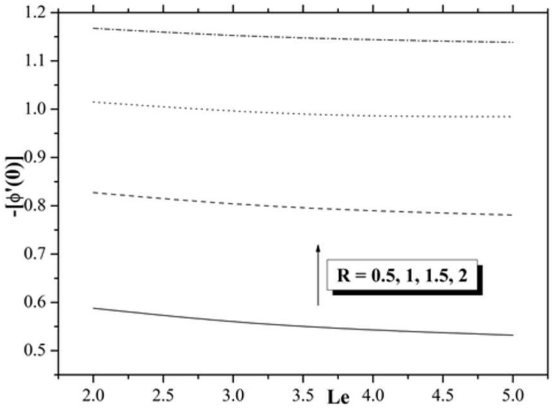

(a)

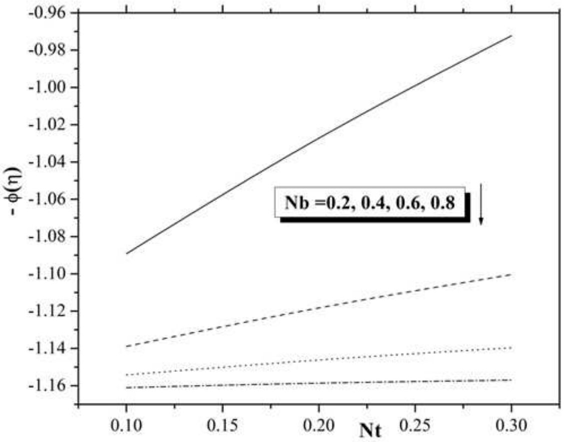

(b)

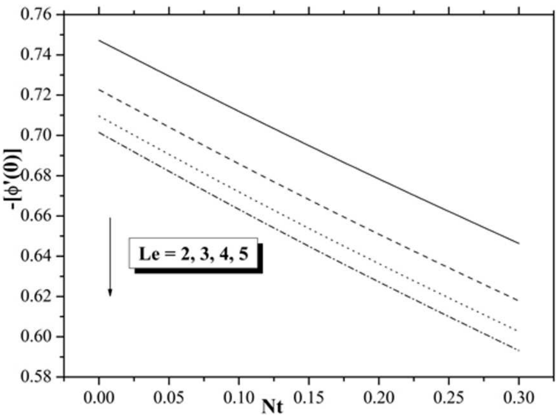

(c)

Figure 11: Influence of Le against R on Sherwood number – a, influence of Nt against Nb on Sherwood number – b, influence of Nt against Le on Sherwood number – c.

agreement. The effects of various parameters on the flow and heat transfer are observed from the graphs and are summarized as follows:

1. Temperature and boundary layer thickness are decreasing functions of the non-uniform heat source sink parameter (A and B).

2. Influence of Brownian motion parameter is to increase the heat transfer rate at the surface and decreases the mass transfer rates.

3. The higher value of Lewis number decreases dimensionless mass transfer rates.

4. A rise in thermophoresis parameter increases temperature and concentration in the boundary layer region

5. Momentum boundary layer thickness reduces due to the influence of Lorenz force.

6. For increasing values of β_1 the momentum boundary layer thickness decreases.

7. The velocity and boundary layer thickness are increasing functions of β_2 and β_2.

8. An increasing the radiation and temperature ratio parameter increases the temperature profile.

9. Thermal boundary layer thickness decreases by increasing the Prandtl number.

Received 7 April 2017

References

[1] Gupta P.S., Gupta A.S.: *Heat and mass transfer on a stretching sheet with suction and blowing.* Can. J. Chem. Eng. **55**(1977), 1, 744–746.

[2] Chan C.K., Char M.I.: *Heat and mass transfer on a continuous stretching sheet with suction and blowing.* J. of Math. Appl. Phys. **135**(1998), 568.

[3] O.D. Makinde, Khan W.A., Khan Z.H.: *Buoyancy effects on MHD stagnation point flow and heat transfer of a nanofluid past a convectively heated stretching/shrinking sheet.* Int. J. Heat Mass Tran. **62**(2013), 526–533.

[4] Rashidi M.M., Rostami B., Freidoonimehr N., Abbasbandy S.: *Free convective heat and mass transfer for MHD fluid flow over a permeable vertical stretching sheet in the presence of the radiation and buoyancy effects.* Ain Shams Eng. J. **5**(2014), 3, 901–912.

[5] Das K.,Sharma R.P., Sarkar A.: *Heat and mass transfer of a second grade magnetohydrodynamic fluid over a convectively heated stretching sheet.* CDE **3**(2016), 4, 330–336.

[6] Ramesh G.K., Gireesha B.J. and Gorla R.S.R.: *Boundary layer flow past a stretching sheet with fluid-particle suspension and convective boundary condition.* Heat Mass Transfer **51**(2015), 8, 1061–1066.

[7] Ramesh G.K., Gireesha B.J., Gorla R.S.R.: *Study on Sakiadis and Blasius flow of Williamson fluid with convective boundary condition.* Nonlinear Engineering **4**(2015), 4, 215–221.

[8] Ramesh G.K., Gireesha B.J.: *Flow over a stretching sheet in a dusty fluid with radiation effect.*J. Heat Transfer ASME **135**(2013), 10, 102702(1-6).

[9] Choi S.U.S., Eastman J.A.: *Enhancing thermal conductivity of fluids with nanoparticles.* Proc. ASME Int. Mech. Eng. Congress and Exposition **66**(1995), 99–105.

[10] Buongiorno J.: *Convective transport in nanofluids.* J. Heat. Trans. – T.ASME **128**(2005), 3, 240–250.

[11] Khan W.A., Pop I.: *Boundary-layer flow of a nanofluid past a stretching sheet.* Int. J. Heat Mass Tran. **53**(2010), 11–12, 2477–2483.

[12] Alsaedi A., Awais M., Hayat T.: *Effects of heat generation/absorption on stagnation point flow of nanofluid over a surface with convective boundary conditions.* Commun. Nonlinear Sci. Numer. Simulat. **17**(2012), 4210–4223.

[13] Rahman M.M., Al-Lawatia M.A., Eltayeb I.A., Al-Salti N.: *Hydromagnetic slip flow of water based nanofluids past a wedge with convective surface in the presence of heat generation (or) absorption.* Int. J. Thermal Sciences **57**(2012), 172–182.

[14] Nandy S.K., Mahapatra T.R.: *Effects of slip and heat generation/absorption on MHD stagnation flow of nanofluid past a stretching/shrinking surface with convective boundary conditions.* Int. J. Heat Mass Tran. **64**(2013), 1091–1100.

[15] Garoosi F., Rohani B., Rashidi M.M.: *Two-phase mixture modeling of mixed convection of nanofluids in a square cavity with internal and external heating.* Powder Technol. **275**(2015), 304–321.

[16] Abolbasharia M.H., Freidoonimehr N., Nazaria F., Rashidi M.M.: *Analytical modeling of entropy generation for Casson nano-fluid flow induced by a stretching surface.* Advanced Powder Technol. **26**(2015), 2, 542–552.

[17] Anwar bég O., Rashidi M.M., Akbari M., Hosseini A.: *Comparative numerical study of single-phase and two-phase models for bionanofluid transport phenomena.* J. Mech. Med. Biol. **14**(2014), 1, 1450011. http://dx.doi.org/10.1142/S0219519414500110.

[18] Rashidi M.M., Nasiri M., Khezerloo M., Laraqid N.: *Numerical investigation of magnetic field effect on mixed convection heat transfer of nanofluid in a channel with sinusoidal walls.* J. Magn. Magn. Mater. **401**(2016), 1, 159–168.

[19] Khalili S., Tamimb H., Khalili A., Rashidi M.M.: *Unsteady convective heat and mass transfer in pseudoplastic nanofluid over a stretching wall.* Adv. Powder Technol. **26**(2015), 5, 1319–1326.

[20] Burgers J.M.: *Mechanical considerations-model systems-phenomenological theories of relaxation and of viscosity.* In: First Report on Viscosity and Plasticity 2nd Edn. (J.M. Burgers Ed.) Nordemann Publishing Company, New York 1935.

[21] Rajagopal K.R., Srinivasa A.R.: *A thermodynamic frame work for rate type fluid models.* J. Non-Newtonian Fluid Mech. **88**(2000), 207–227.

[22] Lee A.R., Markwick A.H.D.: *The mechanical properties of bituminous surfacing materials under constant stress.* J.Soc. Chem. Ind. **56**(1937), 146–156.

[23] Tan B.H., Jackson I., Gerald J.D.F.: *High-temperature viscoelasticity of fine-grained polycrystalline Olivine.* Phys. Chem. Miner. **28**(2001), 9, 641–664.

[24] Khan M. and Khan W.A.: *Forced convection analysis for generalized Burgers nanofluid flow over a stretching sheet.* AIP Adv. **5**(2015), 107138.

[25] Hayat T., Asad S., Alsaedi A.: *Flow of Burger's fluid over an inclined stretching sheet with heat and mass transfer.* J. Cent. South Univ., **22**(2015), 3180–3188.

[26] Ravindran P., Krishnan J.M., Rajagopal K.R.: *A note on the flow of a Burgers fluid in an orthogonal rheometer.* Int. J. Eng. Sci. **42**(2004), 1973–1985.

[27] Quintanilla R., Rajagopal K.R.: *On Burgers fluids.* Math. Meth. Appl. Sci. **29**(2006), 2133–2147.

[28] Fetecau C., Hayat T., Corina Fetecau: *Steady-state solutions for some simple flows of generalized Burgers fluids.* Int. J. Non-linear Mech. **41**(2006), 5, 880–887.

[29] Fetecauc C., Hayat T., Khan M., Fetecau C.: *A note on longitudinal oscillation of a generalized Burgers fluid in a cylindrical domains.* J. Non-Newtonian Fluid Mech. **165**(2010), 350–361.

[30] Khan M.: *Stokes' first problem for an MHD Burgers fluid.* Commun. Theor. Phys. **59**(2013), 99–104.

[31] Khan M., Malik R., Anjum A.: *Exact solutions of MHD second Stokes flow of generalized Burgers fluid.* Appl. Math. Mech.-Engl. Ed. **36**(2015), 211–224.

[32] Shehzad S.A., Hayat T., Alsaedi A., Mustafa A.O.: *Nonlinear thermal radiation in three-dimensional flow of Jeffrey nanofluid: A model for solar energy.* Appl. Math. Comput. **248**(2014), 273–286.

[33] Ramesh G.K.,Roopa G.S., Gireesha B.J., Shehzad S.A., Abbasi F.M.: *An electro-magneto-hydrodynamic flow Maxwell nanoliquid past a Riga plate: A numerical study.* J. Braz. Soc. Mech. Sci. **39**(2017), 11, 4547–4554.

[34] Hayat T., Muhammad T., Alsaedi A., Alhuthali M.S.: *Magnetohydrodynamic three-dimensional flow of viscoelastic nanofluid in the presence of nonlinear thermal radiation.* J. Magn. Magn. Mater. **385**(2015), 222–229.

[35] Ramesh G.K., Prasannakumara B.C., Gireesha B.J., Shehzad S.A., Abbasi F.M.: *Three dimensional flow of Maxwell nanofluid past a bidirectional porous stretching surfacewith thermal radiation.* Thermal Sci. Eng. Progress **1**(2017), 6–14.

[36] Abbas Z., Sheikh M., Motsa S.S.: *Numerical solution of binary chemical reaction on stagnation point flow of Casson fluid over a stretching/shrinking sheet with thermal radiation*. Energy **95**(2016), 12–20.

[37] Turkyilmazoglu M., Pop I.: *Heat and mass transfer of unsteady natural convection flow of some nanofluids past a vertical infinite flat plate with radiation effect.* Int. J. Heat . Mass Tran. **59**(2013), 167–171.

[38] Cortell R.: *A note on magnetohydrodynamic flow of a power-law fluid over a stretching sheet*. Appl. Math. Comput. **168**(2005), 557–566.